Neuron
Review

Amyloid Polymorphism: Structural Basis and Neurobiological Relevance

Robert Tycko[1,*]
[1]Laboratory of Chemical Physics, National Institute of Diabetes and Digestive and Kidney Diseases, National Institutes of Health, Bethesda, MD 20892-0520, USA
*Correspondence: robertty@mail.nih.gov
http://dx.doi.org/10.1016/j.neuron.2015.03.017

Our understanding of the molecular structures of amyloid fibrils that are associated with neurodegenerative diseases, of mechanisms by which disease-associated peptides and proteins aggregate into fibrils, and of structural properties of aggregation intermediates has advanced considerably in recent years. Detailed molecular structural models for certain fibrils and aggregation intermediates are now available. It is now well established that amyloid fibrils are generally polymorphic at the molecular level, with a given peptide or protein being capable of forming a variety of distinct, self-propagating fibril structures. Recent results from structural studies and from studies involving cell cultures, transgenic animals, and human tissue provide initial evidence that molecular structural variations in amyloid fibrils and related aggregates may correlate with or even produce variations in disease development. This article reviews our current knowledge of the structural and mechanistic aspects of amyloid formation, as well as current evidence for the biological relevance of structural variations.

Aberrant aggregation of certain peptides and proteins causes many neurodegenerative diseases, including Alzheimer disease (AD), Parkinson disease (PD), transmissible spongiform encephalopathies (TSEs), Huntington disease, frontotemporal dementia, and amyotrophic lateral sclerosis. The association of protein aggregation with neurodegeneration motivates efforts in many laboratories to elucidate the detailed molecular aspects of protein aggregation, including mechanisms and pathways of aggregation and molecular structures of the aggregated states of the relevant peptides and proteins.

The thermodynamic endpoints of protein aggregation (i.e., the most stable self-assembled states under typical conditions) are often filamentous assemblies called amyloid fibrils. Figure 1 shows examples of amyloid fibrils prepared in vitro. Amyloid fibrils are inherently noncrystalline, insoluble materials, making it difficult to determine their internal molecular structures by traditional methods for high-resolution structure determination, especially X-ray crystallography and multidimensional nuclear magnetic resonance (NMR) spectroscopy. Over the past 10–15 years, progress has been made on the amyloid structure problem through the application of less traditional methods. One of the most powerful methods for structural studies of amyloid fibrils is solid state NMR (ssNMR), which means a set of NMR techniques that are designed specifically for applications to molecular assemblies that are not soluble and not necessarily crystalline (Tycko, 2011). Other methods that have contributed to recent progress include electron paramagnetic resonance (EPR) (Margittai and Langen, 2008), electron microscopy (Goldsbury et al., 2005; Serpell and Smith, 2000), cryo-electron microscopy (cryo-EM) (Jiménez et al., 1999; Meinhardt et al., 2009), and hydrogen/deuterium exchange measurements (Kheterpal et al., 2006; Lührs et al., 2005; Olofsson et al., 2007; Toyama et al., 2007). In addition, X-ray crystallographic studies of peptides in amyloid-like crystals have been quite valuable (Nelson et al., 2005; Sawaya et al., 2007). Detailed structural information at the molecular level is essential for a full understanding of the amyloid formation process, for understanding of biological effects arising from structural variations, and for the rational development of compounds that can inhibit amyloid formation (Estrada and Soto, 2007) or bind specifically to amyloid fibrils for diagnostic imaging (Fleisher et al., 2011; Klunk et al., 2004).

A fundamentally important property of amyloid fibrils is their ability to amplify and propagate their own structures by recruitment of additional protein molecules from their surroundings. Recent studies in a number of laboratories highlight the biomedical significance of amyloid self-propagation in neurodegenerative diseases (Eisele et al., 2010; Frost et al., 2009a; Iba et al., 2013; Kfoury et al., 2012; Langer et al., 2011; Luk et al., 2012a, 2012b; Meyer-Luehmann et al., 2006; Sanders et al., 2014; Stöhr et al., 2012, 2014; Volpicelli-Daley et al., 2011; Watts et al., 2014). Amyloid self-propagation is a likely underlying mechanism for the infectious nature of prion protein (PrP) particles in TSEs (Collinge and Clarke, 2007; Prusiner, 2013). Thus, the self-propagation of amyloid fibrils formed by proteins other than PrP is now often called "prion-like" behavior.

If one accepts the definition that prions are disease-causing, infectious, proteinaceous particles, then in vitro self-propagation should not be called "prion-like." Other issues regarding this term, such as the distinction between propagation within a single organism and transmission between organisms and the distinction between naturally occurring and artificially induced transmission, have been discussed by others (Ashe and Aguzzi, 2013; Hardy and Revesz, 2012).

Polymorphism is another important property of amyloid fibrils (Tycko, 2014). As shown in Figure 1 for the amyloid-β (Aβ) peptide associated with AD and the α-synuclein (α-syn) protein associated with PD, fibrils formed by a single peptide or protein can be polymorphic, i.e., can exhibit multiple distinct

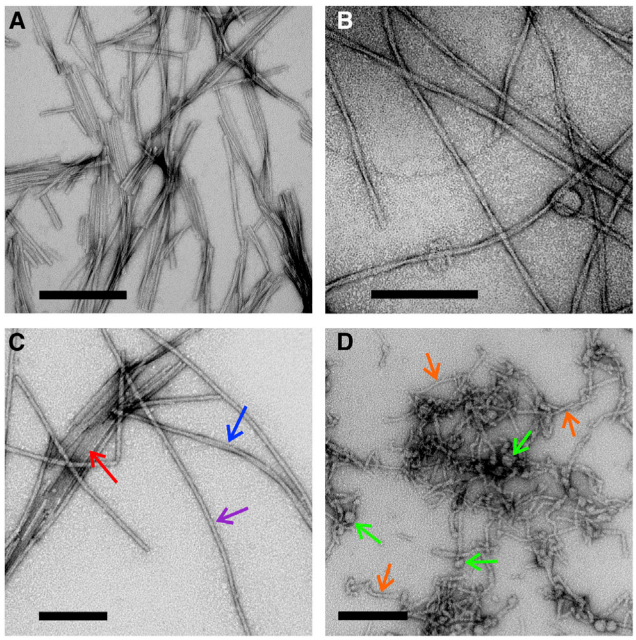

Figure 1. Polymorphism of Amyloid Fibrils and Aggregation Intermediates, as Seen in Transmission Electron Microscope Images with Negative Staining
(A) Synthetic Aβ40 fibrils with "striated ribbon" morphologies.
(B) Synthetic Aβ40 fibrils with "twisted" morphologies.
(C) Recombinant α-synuclein fibrils with striated ribbon (red arrow), twisted (blue arrow), and rod-like (purple arrow) morphologies.
(D) Synthetic Aβ40 aggregation intermediates with protofibrillar (orange arrows) and nonfibrillar (green arrow) morphologies, prepared by quiescent incubation of a 100 μM peptide solution at 24°C and pH7.4 for 36 hr. Scale bars represent 200 nm.

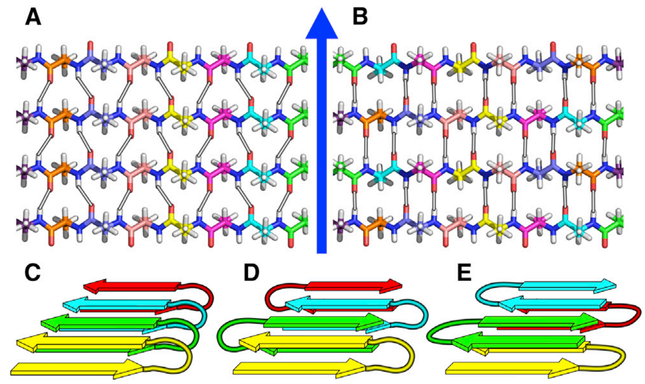

Figure 2. Varieties of Cross-β Structures in Amyloid Fibrils
(A) An "in-register" parallel cross-β structure, in which β strand segments from adjacent protein or peptide molecules align in parallel and with no shift of their amino acid sequences (represented by the varying colors of carbon atoms) relative to one another.
(B) An antiparallel cross-β structure. Silver bars indicated hydrogen bonds between backbone carbonyl and backbone amide groups. The fibril growth direction is indicated by the blue arrow.
(C–E) Schematic representations of cross-β structures that could be formed by a peptide that contains two separate β strand segments, separated by a loop or turn segment. Colors indicate successive copies of the same peptide molecule. From left to right, the structures are a double-layered, in-register parallel cross-β unit, a double-layered antiparallel cross-β unit, and a double-layered antiparallel β-hairpin structure.

appearances in transmission electron microscopy (TEM) images. Although in principle amyloid polymorphs could merely be different bundled arrangements of the same basic amyloid "protofilament" structure, in fact ssNMR measurements clearly show that amyloid polymorphs contain distinct molecular structures, and that each molecular structure can propagate itself (Bousset et al., 2013; Frederick et al., 2014; Gath et al., 2014; Paravastu et al., 2008; Petkova et al., 2005). Self-propagating, molecular-level polymorphism of amyloid fibrils is a likely underlying mechanism for the occurrence of distinct prion strains in TSEs (Collinge and Clarke, 2007; Safar et al., 1998; Toyama and Weissman, 2011; Wickner et al., 2010). As discussed below, recent studies suggest that neurodegenerative diseases such as AD, PD, and tauopathies (involving aggregation of the tau protein) may exhibit variations in clinical characteristics and neuropathology that are attributable to amyloid polymorphism, in analogy to prion strains.

This article reviews recent work on amyloid formation, molecular structure, and polymorphism that relates to the issues described above. Several excellent reviews of relevant experiments in cell cultures and animal models have appeared recently (Ashe and Aguzzi, 2013; Guo and Lee, 2014; Hardy and Revesz, 2012; Jucker and Walker, 2013; Walker et al., 2013). Therefore, this article focuses primarily on physical and structural properties of amyloid fibrils and related aggregates that could be the basis for the biological phenomena. Although this article emphasizes work on Aβ, α-syn, and tau, similar ideas apply to other proteins whose aggregation is associated with neurodegeneration. It should also be noted that amyloid formation has been shown to be a biologically functional, presumably evolved, property of a variety of proteins (Pham et al., 2014).

Principles of Amyloid Formation from In Vitro Studies

Amyloid fibrils are typically 5–15 nm in width, unbranched, straight over length scales approaching 1 micron, and often many microns long. Measurements on bundles of aligned fibrils by X-ray fiber diffraction first revealed that they contain "cross-β" structures (Eanes and Glenner, 1968), which are ribbon-like β sheets in which β strand segments run approximately perpendicular to the fibril growth direction and hydrogen bonds between β strands are approximately parallel to the growth direction (Sunde et al., 1997). Figure 2 shows atomic models of ideal cross-β structures, which can involve either parallel or antiparallel alignments of adjacent β strands. Figure 2 also shows examples of double-layered cross-β structures, as may exist in fibrils formed by peptides or proteins with two separate β strand segments. As discussed below, a single amyloid fibril can contain several cross-β subunits, with two or more β sheet layers within each subunit. The spacing between β strands in a β sheet is always 0.46–0.48 nm. Therefore, a one micron length of amyloid fibril typically contains thousands of protein molecules, with the exact number depending on the number of cross-β subunits, the number of β strand segments contributed to each cross-β subunit by one molecule, and the number of β sheet layers within each subunit.

In vitro, amyloid fibrils are readily prepared from purified synthetic peptides or recombinant proteins by incubation in simple

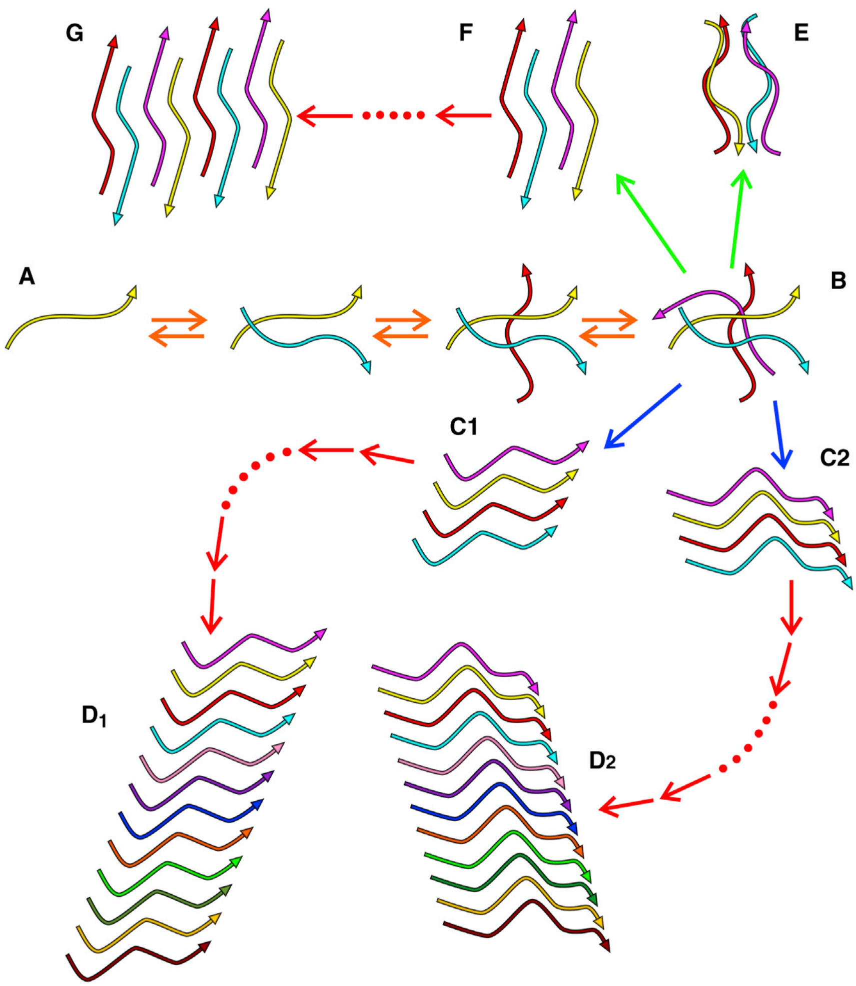

Figure 3. Conceptual Representation of Molecular Mechanisms for Amyloid Formation

Starting with a peptide or protein monomer A, a series of reversible monomer additions (orange arrows) results in a transient oligomer B that can undergo internal structural rearrangements (i.e., nucleation events, blue arrows) to form cross-β-like structures C_1 and C_2. Subsequent monomer additions to C_1 and C_2 (red arrows) result in fibril polymorphs D_1 and D_2. Variations in growth conditions can affect the relative nucleation rates or subsequent growth rates of the two polymorphs. Fibril growth conditions can also affect the rates of fibril fragmentation or secondary nucleation, favoring one polymorph over the other. In real systems, more than two fibril polymorphs can be formed by the same peptide or protein. In addition, fibril nucleation may compete with the formation of "off-pathway" aggregation intermediates (green arrows), such as a metastable oligomer E and a protofibril G, which grows from cross-β-like nucleus F. Once formed, species D_1, D_2, E, and G remain in dynamic equilibrium with monomers (or small oligomers), allowing a net transfer of peptide or protein molecules from the less stable to the more stable species.

aqueous buffers. Typical protein concentrations are in the 10 to 1,000 μM range. Under these conditions, fibrils appear on time scales of minutes to days. In de novo preparations, the total fibril mass often has a sigmoidal dependence on time, with a "lag period" during which the fibril concentration remains too low to be detectable, followed by a rapid rise in concentration to a plateau level, at which the available protein in the solution has been mostly consumed. Fibril growth mechanisms that can lead to such a sigmoidal time-dependence have been investigated by several groups (Chen et al., 2002; Cohen et al., 2013; Knowles et al., 2009; Lomakin et al., 1997). A highly schematic representation of the amyloid formation process, including polymorphism and "off-pathway" aggregation intermediates, is given in Figure 3. Although many details remain uncertain, the general picture is that the protein molecules self-associate transiently into oligomers of various sizes during the lag period until "primary nucleation events" occur, corresponding to the formation of oligomers that are sufficiently stable and have appropriate structures, allowing them to persist and grow into fibrils by the addition of protein molecules to their ends.

Once a small concentration of fibrils has accumulated through primary nucleation, additional fibrils can appear by fragmentation of existing fibrils or, as suggested recently (Cohen et al., 2013), by "secondary nucleation" processes, which may correspond to the initiation of new fibrils along the sides of existing fibrils. The rapid rise of fibril mass after the lag period occurs when fragmentation or secondary nucleation dominates the overall time dependence of protein aggregation.

Amyloid fibril formation is sometimes considered to be an irreversible process. This is incorrect. Even after the mass of fibrils reaches its plateau value, fibrils coexist with a low concentration of soluble protein. Association and dissociation of protein molecules continues to occur at fibril ends, with well-defined "on" and "off" rates as in any protein-protein or ligand-protein binding process at thermal equilibrium. If fibrils are placed in a solution that contains an excess of soluble protein, they grow. Conversely, if fibrils are placed in a solution that contains a deficit of soluble protein, they shrink until the concentration of soluble protein reaches its equilibrium value (Qiang et al., 2013; Wetzel, 2006).

Self-propagation of amyloid fibrils is readily demonstrated in vitro through seeded fibril growth. In this context, fibril "seeds" are short fibril fragments, usually created by sonication of long "parent" fibrils. When seeds are added to a solution of soluble protein, the seeds grow into longer fibrils by addition of protein molecules to their ends. The newly elongated fibrils can then be sonicated to create a second generation of seeds, which can be used in a second round of seeded growth. Fibrils that grow from seeds generally inherit the morphologies (as revealed by TEM) and molecular structures (as revealed by ssNMR) of their parents (Bousset et al., 2013; Kodali et al., 2010; Petkova et al., 2005).

When seeds are added at the beginning of a fibril growth experiment, the lag period is abrogated and the fibril mass increases linearly with time (Qiang et al., 2013; Wetzel, 2006). Agitation or stirring of protein solutions is often found to accelerate the overall growth of fibrils in vitro. This effect is attributable to fibril fragmentation by shear forces, which increases the concentration of fibril ends and hence the net rate of fibril growth. The presence or absence of agitation can also influence the predominant fibril structures that develop (see below).

Self-propagation of prions or prion-like aggregates, such as fibril seeds, is often described as a "templated conformational conversion" process, in which the prion-like aggregates inevitably "corrupt" the structures of soluble proteins they encounter (Collinge and Clarke, 2007; Guo and Lee, 2014; Prusiner, 2013; Walker et al., 2013). This description may be misleading, because a net conversion of protein molecules from their soluble state to their aggregated state (even if accompanied by a conformational change) only occurs if the concentration of soluble molecules exceeds its equilibrium value, i.e., if the solution is supersaturated. Thus, observations that protein aggregation and amyloid formation can be triggered within cells or in mammalian tissue by introduction of exogenous aggregates (Eisele et al., 2010; Frost et al., 2009a; Iba et al., 2013; Kfoury et al., 2012; Langer et al., 2011; Luk et al., 2012a, 2012b; Meyer-Luehmann et al., 2006; Sanders et al., 2014; Stöhr et al., 2012, 2014; Volpicelli-Daley et al., 2011; Watts et al., 2014) imply that the relevant proteins are supersaturated in the intracellular or extracellular compartments where aggregation occurs.

Fibril seeding is often highly sequence-specific. For example, fibrils prepared in vitro from the islet amyloid polypeptide (IAPP) do not act as efficient seeds for Aβ40 fibrils, despite the similarity of their core-forming sequences (O'Nuallain et al., 2004). Fibrils formed in vitro by Aβ40 or by the 42-residue Aβ peptide (Aβ42) do not cross-seed one another efficiently (Lu et al., 2013). However, in certain cases, some of which may be biomedically important (Giasson et al., 2003), efficient cross-seeding has been reported. The factors that determine cross-seeding efficiencies are not understood in detail but presumably have a molecular structural basis. Thus, cross-seeding efficiencies can be polymorph-dependent, as exemplified by the dependence of species barriers to prion infectivity on TSE strains (Jones and Surewicz, 2005).

When fibrils are grown de novo under conditions that produce a heterogeneous mixture of polymorphs, the relative populations of different polymorphs can change in subsequent generations that are produced by successive rounds of seeded growth (Paravastu et al., 2008). This is because different fibril structures can have different self-propagation efficiencies, for example due to different susceptibilities to fragmentation by sonication or due to different intrinsic elongation rates. After many rounds, a nearly homogeneous fibril sample can be created, possibly dominated by a structure that was a minor component of the original parent sample. The predominant structure can depend on the precise details of the seeded growth protocol (Qiang et al., 2011).

Under typical in vitro conditions, various intermediate states of protein aggregation are often observed by TEM or atomic force microscopy (AFM), including assemblies that are roughly spherical (Hoshi et al., 2003; Yu et al., 2009), assemblies that are doughnut-shaped or pore-like (Lasagna-Reeves et al., 2011), and assemblies called "protofibrils" that are fibril-like, but are shorter and more highly curved than mature amyloid fibrils (Goldsbury et al., 2005; Williams et al., 2005). Examples of Aβ40 aggregation intermediates are shown in Figure 1D. These intermediates may develop during the lag period, before fibrils appear in detectable quantities, and are generally less stable thermodynamically than mature amyloid fibrils. Nonetheless, under certain conditions, aggregation intermediates can persist as the predominant structural state for many hours or days, allowing characterization of their structural properties and biological effects (Ahmed et al., 2010; Chimon and Ishii, 2005; Chimon et al., 2007; Kheterpal et al., 2006; Ladiwala et al., 2012; Lopez del Amo et al., 2012; Qiang et al., 2012; Sandberg et al., 2010; Sarkar et al., 2014; Scheidt et al., 2011, 2012; Tay et al., 2013).

Experiments from many laboratories provide evidence that aggregation intermediates can be important neurotoxic species in neurodegenerative diseases. Although it is sometimes stated that amyloid fibrils are not toxic in cell cultures, experimental results from several groups show that this is not true (Chimon et al., 2007; Petkova et al., 2005; Qiang et al., 2012; Resende et al., 2008; Xue et al., 2009). The apparent toxicity of fibrils in cell cultures depends on their state of self-association and/or their lengths, with sonicated fibrils being more toxic than long fibrils that form entangled masses (Petkova et al., 2005; Xue et al., 2009). The relationship between inherent cytotoxicity and molecular structure (e.g., cross-β versus non-cross-β structure, parallel β sheet versus antiparallel β sheet structure) is not yet clear. The possibility that fibril toxicity is attributable to non-fibrillar assemblies that develop from fibrils in the culture medium can be dismissed for several reasons: (1) in general, more thermodynamically stable species do not spontaneously evolve toward less stable species, (2) development of non-fibrillar assemblies from fibrils is not observed in images of dissolving fibrils (Qiang et al., 2013), (3) non-fibrillar assemblies are not detectable in spectroscopic and antibody-binding experiments on short, cytotoxic fibril preparations (Xue et al., 2009).

In animal models, strong evidence exists that oligomeric aggregates have adverse effects on neuronal function and memory (Lesné et al., 2006, 2013; Shankar et al., 2008; Walsh et al., 2002). In the case of AD, immunohistochemical studies show that certain oligomeric species exist in human brain tissue (Kayed et al., 2003; Noguchi et al., 2009), although the molecular structural properties of these species remain to be elucidated. At least some of these species may be fibril fragments (Tomic et al., 2009). In AD, it is conceivable that both fibrillar and non-fibrillar aggregates contribute to neurodegeneration, perhaps through different mechanisms. Recent progress on the structural characterization of aggregation intermediates is discussed below.

Molecular Structural Basis for Amyloid Polymorphism

Whereas X-ray fiber diffraction patterns and TEM images provide important information about amyloid structures, one cannot determine the molecular structures within amyloid fibrils or even prove that well-defined, ordered structures exist based on these data. In particular, the identities of β strand segments, the types of β sheets (parallel versus antiparallel intermolecular alignment), the nature of interactions between β sheet layers, the conformations of non-β strand segments, and other structural features cannot be determined. This information is available from ssNMR measurements, which show that amyloid fibrils do indeed contain well-defined molecular and supramolecular structures (Bertini et al., 2011; Lu et al., 2013; Paravastu et al., 2008; Petkova et al., 2006; Van Melckebeke et al., 2010). X-ray crystallography of peptides that crystallize into cross-β structures also provides a wealth of detailed information about intermolecular interactions within such structures (Nelson et al., 2005; Sawaya et al., 2007).

Molecular structural information is contained in several types of ssNMR measurements. NMR chemical shifts (i.e., the precise values of NMR frequencies) have strong dependences on local molecular conformation that can be analyzed by comparisons with chemical shift databases for proteins with known structures (Shen et al., 2009). Pairwise distances between atomic nuclei can be determined precisely by quantitative measurements of nuclear magnetic dipole-dipole couplings or approximately by detection of "crosspeak" signals that connect the corresponding pairs of NMR frequencies in multidimensional ssNMR spectra (De Paëpe, 2012). Other types of ssNMR measurements can also be used to obtain structural constraints at various length scales (Franks et al., 2008; Sengupta et al., 2013). Strong, sharp signals in ssNMR spectra arise from structurally ordered, relatively rigid protein segments, while disordered and highly flexible segments generally do not contribute to the ssNMR spectra (Van Melckebeke et al., 2010). Thus, segments that comprise the core structure of an amyloid fibril can be distinguished from flexible loops or tails, which are generally outside the core. For protein assemblies such as amyloid fibrils, ssNMR data are often combined with constraints from electron microscopy or other sources. Computational approaches are then used to develop molecular structural models that are consistent with the available data.

In the case of Aβ fibrils, initial ssNMR studies focused on fibrils formed by nine-residue and 26-residue synthetic peptides representing residues 34–42 ($A\beta_{34-42}$) and 10–35 ($A\beta_{10-35}$) of full-length Aβ (Benzinger et al., 1998; Lansbury et al., 1995). The peptides were synthesized with ^{13}C labels at specific carbon sites, and ssNMR methods were used to determine specific intermolecular and intramolecular distances among the labeled carbon sites. Results for $A\beta_{34-42}$ indicated a cross-β structure comprised of antiparallel β sheets (Lansbury et al., 1995); results for $A\beta_{10-35}$ indicated a cross-β structure comprised of parallel β sheets in which individual peptide molecules align with their neighbors in an "in-register" manner (Benzinger et al., 1998). These results were the first definite experimental indication that cross-β motifs within fibrils formed by a given peptide or protein have specific supramolecular structures and that structures within fibrils formed by different peptides can be qualitatively different from one another.

Subsequent ssNMR and EPR measurements on fibrils formed in vitro by full-length Aβ (Aβ40 and Aβ42) showed that these fibrils also contain in-register parallel β sheets (Antzutkin et al., 2000, 2002; Balbach et al., 2002). Experiments by Petkova et al. then showed that Aβ40 fibril morphologies can be controlled reproducibly by subtle variations in growth conditions in vitro (Petkova et al., 2005). Specifically, Aβ40 fibrils grown at 24°C and pH7.4 with gentle agitation of the Aβ40 solution during the growth period have a predominant "striated ribbon" morphology (Figure 1A), whereas fibrils grown under the same conditions except without agitation have a predominant "twisted" morphology (Figure 1B). Moreover, solid-state NMR spectra of striated ribbons are obviously different from spectra of twisted fibrils, with many differences in the ^{13}C NMR chemical shifts (i.e., the precise ^{13}C NMR frequencies) of individual ^{13}C-labeled carbon sites (Petkova et al., 2005). Since NMR chemical shifts are sensitive to local molecular conformation and structural environment, these results prove that distinct fibril morphologies correspond to distinct underlying molecular structures. The number of distinct Aβ40 fibril polymorphs is at least five, according to subsequent studies, and may be on the order of ten (Bertini et al., 2011; Kodali et al., 2010; Lu et al., 2013; Meinhardt et al., 2009; Niu et al., 2014).

The molecular-level polymorphism observed in Aβ40 fibrils has also been observed in ssNMR studies of amyloid fibrils formed by other disease-associated peptides and proteins, including IAPP (Luca et al., 2007), α-syn (Bousset et al., 2013; Comellas et al., 2011; Heise et al., 2005, 2008; Lemkau et al., 2012), and tau (Andronesi et al., 2008; Daebel et al., 2012; Frost et al., 2009b). Thus, in general, molecular structures within amyloid fibrils formed in vitro are not determined uniquely by the amino acid sequences of amyloid-forming peptides and protein. Instead, they are determined by the precise details of growth conditions.

In principle, different fibril polymorphs can have different spontaneous nucleation rates, extension rates, fragmentation rates, and secondary nucleation rates, resulting in the observed dependence of the predominant fibril morphology on growth conditions. For Aβ40, the predominance of striated ribbon fibrils under agitated growth conditions is attributable in part to the greater susceptibility of striated ribbons to fragmentation by shear forces (Qiang et al., 2013).

Full molecular structural models for striated ribbon and twisted Aβ40 fibrils, shown in Figures 4A and 4B, were developed from combinations of structural constraints from ssNMR and electron microscopy (Paravastu et al., 2008; Petkova et al., 2006). These models represent the first case in which specific molecular structural features that differentiate one polymorph from another were identified. Because striated ribbons contain variable numbers of protofilaments (see Figure 1A), the model for striated ribbons represents the structure of one protofilament. Somewhat surprisingly, ssNMR data indicate that the peptide conformations within the two polymorphs are quite similar, consisting of two β strand segments (residues 10–22 and 30–40, roughly) that are preceded by a disordered segment (residues 1–9) and separated by a bend or loop (residues 23–29). The β strand segments participate in separate parallel β sheets, which interact through contacts among hydrophobic amino acid sidechains. The principal difference between the two polymorphs is their overall symmetry, with the striated ribbon protofilament containing two cross-β subunits, related by approximate 2-fold rotational symmetry about the fibril growth axis, and the twisted fibril containing three cross-β units, related by approximate 3-fold rotational symmetry. In addition, the detailed conformations of the bend segments differ in the two polymorphs. The bend segment within 2-fold symmetric striated ribbon protofilaments is bridged by an

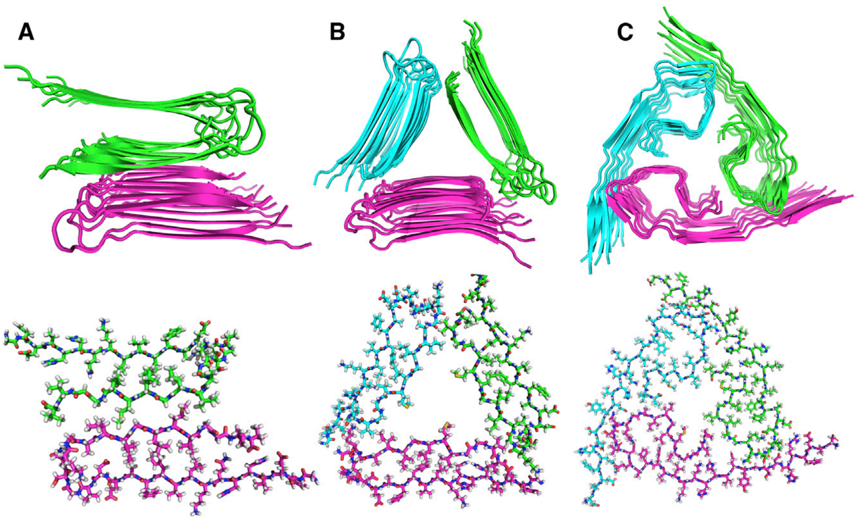

Figure 4. Molecular Structural Models for Three Aβ40 Fibril Polymorphs, Based on Data from ssNMR and Electron Microscopy
(A) Fibrils grown in vitro with the striated ribbon morphology, as in Figure 1A.
(B) Fibrils grown in vitro with the twisted morphology, as in Figure 2B.
(C) Fibrils derived from brain tissue of a patient with AD. In each case, the fibril structure is viewed in cross-section, with the fibril growth direction approximately perpendicular to the page.
Upper parts are cartoon representations, with colors indicating the different cross-β subunits within 2-fold symmetric (A) or 3-fold symmetric (B and C) structures. Eight Aβ40 molecules are shown in each subunit. Lower parts are atomic representations, with one molecule in each subunit. Residues 9–40 are shown in (A) and (B). Residues 1–40 are shown in (C). Models in (A)–(C) are based on PDB: 2LMN, 2LMP, 2M4J.

electrostatic interaction between oppositely charged side chains of Asp23 and Lys28 (i.e., a salt bridge interaction). This interaction is absent in 3-fold symmetric twisted fibrils.

At least two other Aβ40 fibril polymorphs, grown under different conditions and with different morphologies in TEM images, have been characterized subsequently by ssNMR. Fibrils grown with vigorous agitation at 37°C and pH8.5 are reported to have a 2-fold symmetric structure, similar to that in Figure 4A, but with somewhat different contacts among amino acid sidechains within and between the two cross-β subunits and with an additional β strand segment in the N-terminal tail (Bertini et al., 2011). Fibrils grown with gentle agitation in the presence of phospholipid vesicles at 37°C and pH7.4 are reported to contain a peptide conformation similar to the conformations in Figures 4A and 4B, but with additional kinks at glycine sites in residues 30–40 (Niu et al., 2014). A detailed structural model for fibrils formed in vitro by the disease-associated Glu22-deletion mutant of Aβ40 has also been reported, according to which the fibrils have 2-fold symmetry, parallel β sheets within the two cross-β units, and a rather intricate conformation for residues 21–40 (Schutz et al., 2014).

It therefore appears that, at least in the case of Aβ40 fibrils, different self-propagating polymorphs have closely related structures, all of which contain in-register parallel β sheets and essentially the same sets of residues on the exterior and in the interior of the fibrils. The number of cross-β subunits can vary, as can the conformations at certain residues, especially residues that form non-β strand segments, as well as the extent of disordered segments. Details of the packing of amino acid sidechains in the interior are also variable.

While the ratio of Aβ40 to Aβ42 is typically around 5:1 in cerebrospinal fluid of normal individuals (Spies et al., 2010), the insoluble Aβ in AD brain tissue is often predominantly Aβ42 (Gravina et al., 1995). Full structural models for Aβ42 fibrils based on ssNMR data have not yet been published. Aβ42 fibrils prepared in vitro have similar morphologies to Aβ40 fibrils, contain parallel β sheets that interact through similar hydrophobic contacts, and may also exist as both 2-fold symmetric and 3-fold symmetric polymorphs (Antzutkin et al., 2002; Lührs et al., 2005; Olofsson et al., 2007; Sato et al., 2006; Török et al., 2002).

Full structural models for α-syn and tau fibrils have also not been published yet, although it is known that both α-syn and tau fibrils contain in-register parallel β sheets (Chen et al., 2007; Der-Sarkissian et al., 2003; Margittai and Langen, 2004), as do amyloid fibrils formed by PrP, and other proteins (Bedrood et al., 2012; Cobb et al., 2007; Helmus et al., 2011; Kryndushkin et al., 2011; Ladner et al., 2010; Luca et al., 2007; Shewmaker et al., 2006; Tycko et al., 2010; Wickner et al., 2008). Wild-type α-syn fibrils prepared in vitro exhibit polymorphisms analogous to those described above for Aβ40 fibrils. As shown in Figure 1C, distinct morphologies can be observed when fibrils are grown under a single set of conditions (Heise et al., 2005). With careful control of growth conditions, a single predominant morphology can be created (Comellas et al., 2011). Wild-type α-syn fibrils that resemble either striated ribbon or twisted Aβ40 fibrils in TEM images (despite the fact that α-syn is a substantially larger protein, containing 140 amino acids) can be created by varying the ionic strength of the α-syn solution, with other conditions being nominally identical (Bousset et al., 2013; Gath et al., 2014). NMR and EPR data indicate that α-syn fibril structures contain both rigid protein segments, which are primarily β strands, and segments that remain disordered and flexible. The locations and lengths of the rigid segments can vary significantly among different polymorphs (Bousset et al., 2013; Gath et al., 2014). Fibrils formed by disease-associated mutants of α-syn have also been examined by ssNMR (Heise et al., 2008; Lemkau et al., 2012, 2013). Structures of these fibrils are qualitatively similar to those formed by wild-type α-syn, but can have somewhat different β strand lengths and locations.

Less is known about structural variations within full-length tau fibrils, as ssNMR studies have been reported only for a 99-residue tau construct called K19, which contains three of the four possible repeat segments (R1, R3, and R4) from the C-terminal portion of full-length tau. Polymorphism in K19 fibrils has not been addressed explicitly, but two different studies of K19 fibrils led to different conclusions regarding the extent of

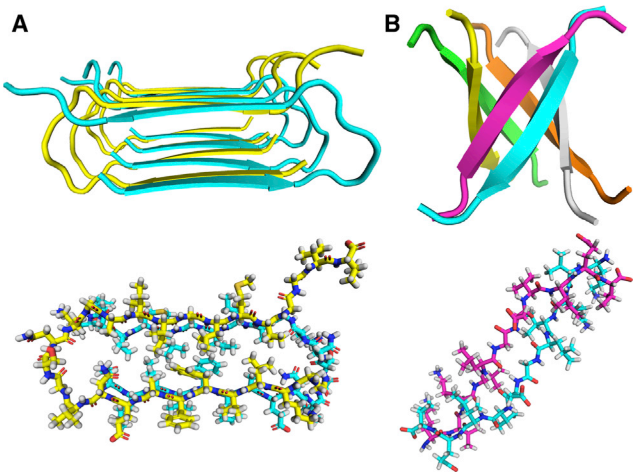

Figure 5. Molecular Structural Models for Two Types of Aggregation Intermediates
(A) Protofibrils formed by D23N-Aβ40, viewed in cross-section, with the protofibril growth direction approximately perpendicular to the page. The cartoon representation (upper part) shows eight D23N-Aβ40 molecules in a double-layered antiparallel cross-β structure identified by ssNMR, with alternating colors to clarify the antiparallel alignment of adjacent molecules. The atomic representation (lower part) shows two adjacent molecules.
(B) Cylindrin oligomer formed by the peptide KVKVLGDVIEV, which derives from the amino acid sequence of αB-crystallin. In the cartoon representation (upper part), the 3-fold symmetry axis of the cylindrin lies vertically in the page and colors indicate different peptide molecules within the hexameric structure. The atomic representation (lower part) shows one pair of antiparallel molecules. Models in (A) and (B) are based on PDB: 2LNQ, 3SGO.

the structurally ordered segments (Andronesi et al., 2008; Daebel et al., 2012). In one study, the structured core of the fibrils was found to contain only a single 18-residue segment, possibly divided into three β strands that are separated by short bends (Daebel et al., 2012). A similar phenomenon was seen in ssNMR studies of fibrils formed by the Tyr145-Stop mutant of human PrP, for which the structured core was found to contain only a single 30-residue segment near the C terminus (Helmus et al., 2008, 2010, 2011).

Experiments on tau fibrils formed in vitro have shown that fibrils prepared de novo from microtubule-binding regions of wild-type tau or disease-associated mutants exhibit different Fourier-transform infrared spectra, different degrees of susceptibility to protease cleavage, and different susceptibilities to fragmentation (Aoyagi et al., 2007; Frost et al., 2009b; von Bergen et al., 2000). When mutant fibrils are used to seed the growth of wild-type fibrils, the resulting wild-type fibrils have the properties of the mutant fibril seeds (Frost et al., 2009b), showing that structural variations are not attributable solely to amino acid sequence variations.

Structures of Aggregation Intermediates

Figure 1D shows aggregation intermediates formed by Aβ40 in vitro. Given that these intermediates have morphologies that are qualitatively different from those of mature fibrils, one might expect their molecular structures also to be qualitatively different. Surprisingly, solid-state NMR data reported to date for Aβ40 and Aβ42 intermediates, prepared under a variety of conditions and exhibiting a variety of morphologies, indicate that the peptide conformations within these intermediates are rather similar to conformations within mature fibrils. In particular, similar identities of β strand segments have been identified, although the β strand segments may be shorter and the overall degree of structural order is lower (Ahmed et al., 2010; Chimon and Ishii, 2005; Chimon et al., 2007; Ladiwala et al., 2012; Lopez del Amo et al., 2012; Qiang et al., 2012; Sarkar et al., 2014; Scheidt et al., 2011, 2012; Tay et al., 2013). Evidence for parallel intermolecular alignments has been obtained in the case of large Aβ40 oligomers with a spherical appearance in TEM images (Chimon et al., 2007). In other cases, ssNMR data argue against a parallel alignment (Ahmed et al., 2010; Tay et al., 2013) or indicate conformational differences (Scheidt et al., 2011, 2012).

Detailed structural characterization of aggregation intermediates is complicated by their greater disorder (relative to mature fibrils), their transient or unstable nature, and the difficulty of preparing morphologically homogeneous samples. To date, only one complete structural model for an Aβ intermediate has been reported, namely that of protofibrils formed by D23N-Aβ40. In this case, it was found that typical de novo fibril growth conditions lead to a mixture of long, straight, mature fibrils (which contain parallel β sheet structures similar to those in Figure 4) and shorter, more highly curved protofibrils with anomalous structures (Tycko et al., 2009). Protofibrils disappeared in seeded growth experiments or when the original mixture was sonicated, indicating the lower thermodynamic stability of protofibrils relative to fibrils. Once a protocol for purifying the protofibrillar aggregates was devised, ssNMR and electron microscopy measurements led to the structural model in Figure 5A (Qiang et al., 2012). Remarkably, this D23N-Aβ40 protofibril structure contains a strand-bend-strand peptide conformation that closely resembles the conformation in Aβ40 fibrils. The same sets of amino acid sidechains from the two β strand segments interact through favorable hydrophobic contacts. However, the two β strand segments form two separate layers of antiparallel β sheets (as in Figure 2D), rather than the two layers of parallel β sheets (as in Figure 2C) seen in mature fibrils.

Crystallographic studies of an 11-residue amyloid-forming peptide from αB crystallin have produced the first atomic-resolution structure of a small, nonfibrillar, oligomeric aggregation intermediate (Laganowsky et al., 2012). This structure, shown in Figure 5B and termed a "cylindrin," consists of six copies of the peptide, arranged as three antiparallel β sheet dimers with 3-fold symmetry about a narrow central pore.

It is conceivable, although not yet proven, that the structures in Figure 5 represent generic motifs for protofibrillar and nonfibrillar intermediates in amyloid formation. It is interesting that both structures involve antiparallel β sheets, whereas the amyloid fibrils formed by proteins associated with neurodegenerative diseases contain parallel β sheets. It is difficult to imagine how conversion from antiparallel to parallel β sheets could occur directly within an aggregated structure because this would require disruption of numerous intermolecular hydrogen bonds and would be disfavored by steric clashes within the structure. Therefore, conversion of these aggregation intermediates to amyloid fibrils must involve dissociation of peptide molecules from the antiparallel structures, followed by their addition to parallel structures. In other words, the antiparallel structures must be off-pathway intermediates. Under certain conditions, they may form more quickly than amyloid fibrils and be sufficiently stable to accumulate and become observable. However, they appear to be structural side-products, rather than obligate precursors to amyloid fibrils. Of course, this does not imply that they are biologically irrelevant.

Intermediate structures that are qualitatively different from those in Figure 5 can also exist, but have not been characterized in detail yet. Some of these may involve parallel intermolecular alignment (Chimon et al., 2007), and some may be "on-pathway," i.e., able to convert directly to an amyloid structure without dissociating. Härd and coworkers have proposed that certain Aβ oligomers contain β-hairpins, based on their observation of a β-hairpin conformation for Aβ40 when bound to an antibody-mimetic protein (Hoyer et al., 2008) and on the enhanced stability of Aβ40 and Aβ42 oligomers when intramolecular disulfide cross-links are introduced in a manner that should stabilize β-hairpins (Sandberg et al., 2010). While a β-hairpin conformation contains two β strands, it differs from the Aβ conformations in Figures 4A, 4B, and 5A in that the two β strands of a β-hairpin interact through backbone hydrogen bonds (as in Figure 2E), rather than through contacts among their sidechains.

Efforts to determine additional intermediate structures are underway in many labs, and we can expect significant progress on this problem in the near future. As one example, cryo-EM has been used to elucidate the tubular structure of Aβ42 protofibrils that bind to PrP and exhibit PrP-dependent inhibition of long-term potentiation (Nicoll et al., 2013). Information of a more qualitative nature about structures of aggregation intermediates has also been obtained from experiments with conformation-dependent antibodies that preferentially recognize certain classes of structures (Kayed et al., 2003; Wu et al., 2010). These antibodies have been used to identify the presence of both nonfibrillar (Lasagna-Reeves et al., 2011) and fibrillar oligomers (Tomic et al., 2009) in AD brain tissue.

Biological Significance of Structural Variations in Amyloid Fibrils and Related Assemblies

Variations in the time course, clinical presentation, and neuropathology of AD are known to exist (Karantzoulis and Galvin, 2011; Lam et al., 2013). The same is true of PD and tauopathies (Dickson et al., 2010; Hughes et al., 1993; Schneider et al., 1997). Do variations in the molecular structural details of amyloid fibrils or aggregation intermediates play a role in the observed variations in neurodegenerative disease development? It is well established that structural variations in infectious PrP aggregates produce distinct TSE strains (Collinge and Clarke, 2007; Prusiner, 2013), although the molecular structures of infectious PrP aggregates have not yet been characterized in detail. Different TSE strains exhibit different incubation periods, different neuropathology, different barriers to interspecies transmission, and different clinical presentations. PrP aggregates from different strains exhibit different patterns of proteolytic cleavage, different degrees of resistance to denaturation, and different spectroscopic signatures (Caughey et al., 1998; Safar et al., 1998; Telling et al., 1996). Prions of yeast also exhibit distinct "weak" and "strong" strains, characterized by different degrees of inactivation of the corresponding yeast prion protein attributable to its aggregation. Yeast prions are known to be amyloid fibrils comprised of parallel β sheet structures (Kryndushkin et al., 2011; Shewmaker et al., 2006; Taylor et al., 1999). Distinct strains may arise from different combinations or lengths of β-sheet-forming protein segments (Toyama et al., 2007).

In the context of AD, there are two separate parts to the question of whether structural variations in aggregated Aβ species have biological effects. The first part is whether different classes of Aβ assemblies (i.e., fibrils, protofibrils, various types of oligomers) have different effects. This is quite plausible because different types of assemblies can contribute to neurodegeneration through different mechanisms, such as membrane disruption (Lasagna-Reeves et al., 2011), interaction with specific cell-surface receptors (Nicoll et al., 2013), interference with synapse function (Li et al., 2009), induction of inflammation (Cunningham, 2013), or generation of reactive oxygen species through metal binding (Eskici and Axelsen, 2012). Although there is strong evidence that nonfibrillar Aβ aggregates have neurodegenerative effects, the stereotypical spreading of neuropathology through brain tissue in AD (Thal et al., 2002) and the ability of exogenous Aβ aggregates to induce neuropathology (Eisele et al., 2010; Langer et al., 2011; Meyer-Luehmann et al., 2006; Morales et al., 2012; Rosen et al., 2012; Stöhr et al., 2012, 2014; Watts et al., 2014) strongly suggests that fibrillar aggregates are also important, as fibrils have the intrinsic capacity to propagate themselves through breakage and regrowth (i.e., through self-seeding).

The second part of the question is whether the molecular-level polymorphism of Aβ fibrils discussed above is biologically significant. It is possible that the biological effects of all fibril polymorphs are nearly indistinguishable. However, one can readily imagine how structural variations in amyloid fibrils might lead to variations in biological effects, for example through structure-specific differences in interactions with cell membranes or cell-surface receptors, differences in binding of metal ions, differences in susceptibility to fragmentation and subsequent transport through tissue, or differences in the structures of oligomeric species that may be derived from or coexist with the fibrils. Although experimental evidence that amyloid fibril polymorphism is important in AD is not yet conclusive, several lines of evidence now exist, as summarized in the following paragraphs.

Aβ fibril fragments have been shown to be toxic in primary neuronal cell cultures at peptide concentrations above 1 μM (Petkova et al., 2005; Qiang et al., 2012). A side-by-side comparison of Aβ40 fibrils prepared in vitro with either striated ribbon or twisted morphologies and with similar lengths showed that the twisted fibrils were significantly more toxic (Petkova et al., 2005), possibly indicating differences in interactions with cell membranes or cell-surface receptors.

Although detailed structural measurements by solid state NMR or related methods cannot be performed directly on amyloid fibrils in brain tissue, such measurements can be performed on fibrils that are prepared by seeded growth from amyloid-containing tissue. Seeded growth amplifies the quantity of fibrils to the milligram scale required for ssNMR and allows the introduction of the necessary ^{13}C and ^{15}N labels (Paravastu et al., 2009).

A recent study compared solid state NMR and electron microscopy data for Aβ40 fibrils seeded with amyloid-enriched extract from brain tissue of two patients with AD and different clinical histories (Lu et al., 2013). For each patient individually, the data indicated a single predominant fibril structure throughout the cerebral cortex. However, ssNMR spectra of fibrils derived from brain tissue of the two patients were clearly different, indicating different predominant structures in the two patients. For one of the patients, an extensive set of ssNMR data was obtained, leading to the detailed molecular structural model shown in Figure 4C. This structure is similar to the 3-fold-symmetric structure of twisted Aβ40 fibrils prepared in vitro (Figure 4B), but contains the Asp23-Lys28 salt bridge of striated ribbon fibrils (Figure 4A), has a structurally ordered N-terminal segment, and includes a more intricate conformation for residues 30–40 than observed in twisted or striated ribbon fibrils. A full structural model for brain-seeded Aβ40 fibrils from the second patient with AD has not yet been reported, but the published data indicate a 3-fold-symmetric structure with specific differences in peptide backbone conformation and inter-residue contacts relative to the model in Figure 4C (Lu et al., 2013). These results establish the important facts that individual AD patients can develop structurally homogeneous Aβ fibrils in their cortical tissue (despite the pronounced propensity for polymorphism indicated by in vitro experiments) and that different patients can develop different fibril structures. Further experiments are required to establish definite correlations between fibril structure and clinical history. In addition, it has not yet been shown that observations for brain-seeded Aβ40 fibrils can be extended to fibrils formed by Aβ42.

Further evidence for possible effects of Aβ fibril structure on disease development comes from experiments with transgenic (Tg) mice that overexpress the human amyloid precursor protein (APP), from which Aβ peptides are generated. In groundbreaking experiments, Walker and colleagues showed that the development of amyloid plaques in cortical tissue of these mice can be accelerated by injection of exogenous amyloid-containing material, either into the brain or elsewhere in the body (Eisele et al., 2010; Langer et al., 2011; Meyer-Luehmann et al., 2006). Thus, Aβ aggregates can exhibit prion-like infectivity, at least under laboratory conditions. Moreover, in experiments in which brain homogenates from AD patients or from two different Tg mouse lines were used, it was found that the patterns of amyloid deposition were dependent on the source of the brain homogenate, suggesting that different homogenates contained different fibril structures that propagated differently through the brain tissue of the recipient mice (Meyer-Luehmann et al., 2006).

Recent experiments by Prusiner and colleagues (Stöhr et al., 2012, 2014) have shown that amyloid deposition in Tg mice can be induced not only by injection of amyloid-containing brain homogenates or extracts, but also by injection of synthetic Aβ fibrils. Differences in Aβ plaque sizes and densities were noted, depending on the conditions under which the synthetic Aβ fibrils were prepared and thus presumably on the molecular structures of the injected fibrils. Additional experiments on Tg mice using brain homogenates from patients with familial AD (Watts et al., 2014) revealed differences in the morphologies of the induced amyloid deposits around cerebral blood vessels and in the relative proportions of 38-residue, 40-residue, and 42-residue Aβ components in these deposits, depending on the nature of the genetic mutations carried by the patients.

Experiments described above used Tg mice that eventually develop Aβ plaques spontaneously, although the appearance of plaques is accelerated significantly by injection of the exogeneous Aβ-containing material. It has also been shown that injection of AD brain homogenate can induce plaque formation in Tg mice and Tg rats that do not develop plaques within their normal life spans (Morales et al., 2012; Rosen et al., 2012).

Related evidence that amyloid polymorphism can have biological significance has been reported for both α-syn and tau fibrils. Experiments by Diamond and colleagues have shown that intracellular aggregation of tau in cell cultures is inducible by exogenous tau fibrils contained in liposomes and persists through many cycles of cell division (Frost et al., 2009a; Kfoury et al., 2012). Cells exposed to exogenous tau fibrils were found to contain distinct sizes of tau aggregates with distinct patterns of proteolysis, representing distinct prion-like strains. Cell lysates were then used to induce tau aggregation in brains of Tg mice, with different lysate strains producing different patterns of tau deposition and microglia activation in the brain tissue (Sanders et al., 2014). These neuropathologic differences in the mice were propagated through several passages. Tau aggregation in Tg and wild-type mice can also be induced by injection of brain homogenates from human patients with various tauopathies. The resulting tau lesions in the mouse brains exhibit variations that correlate with neuropathologic variations in the original human tissue (Clavaguera et al., 2013).

In the case of α-syn, polymorphs similar to the twisted and striated ribbon polymorphs of Aβ40 fibrils can be prepared in vitro by growing the α-syn fibrils in buffers with either low or high ionic strengths (Bousset et al., 2013). The two polymorphs have different antibody-binding properties and (according to ssNMR data) different combinations of structurally ordered and disordered segments (Gath et al., 2014). Both polymorphs can induce intracellular aggregation of α-syn in neuronal cell cultures, but with different rates and different degrees of self-propagation stability.

Intracellular α-syn fibril formation in primary neuronal cell cultures from mice and rats has been shown to occur after exposure to sonicated fibril fragments formed by full-length recombinant human α-syn or by truncated constructs containing the central hydrophobic segment of α-syn (Volpicelli-Daley et al., 2011). It is not known whether the induced intracellular α-syn fibrils have the same structures in all cases. In these experiments, exogenous fibril fragments were found to enter the neurons by adsorptive endocytosis, initially producing intracellular aggregation in axons and subsequently leading to the appearance of α-syn fibrils in cell bodies and dendrites. When pre-formed recombinant fibrils were injected into wild-type mouse brains, aggregated α-syn was found to spread from the injection site exclusively to axonally connected brain regions (Luk et al., 2012a).

Although cross-seeding of amyloid fibril formation is generally inefficient between proteins with different amino acid sequences, α-syn and tau fibrils have been shown to cross-seed one another (Giasson et al., 2003). When recombinant α-syn fibrils are grown de novo under certain conditions, these fibrils do not induce intracellular tau aggregation in cultured neurons. However, after ten rounds of seeded growth, the resulting α-syn fibrils do induce intracellular tau aggregation, presumably due to preferential amplification of a specific α-syn fibril structure by repeated seeding as discussed above (Guo et al., 2013). Indeed, infrared and circular dichroism spectra of the seeded fibrils were found to differ from spectra of the de novo fibrils, as did their protease digestion patterns. When the same fibrils were injected into Tg mice that overexpress a human tau mutant, accelerated tau aggregation was observed only with the seeded α-syn fibrils, indicating a significant structurally based difference in pathological cross-seeding efficiencies within brain tissue.

Conclusions

Our understanding of amyloid fibril structures and structural variations has advanced substantially in recent years, due to information from ssNMR and other novel experimental approaches. Structures of various classes of aggregation intermediates are now being elucidated. Although the existence of significant correlations between variations in molecular structural features and variations in neurodegenerative diseases in humans has not been proven, this possibility now seems quite plausible and worth pursuing in future studies. Such correlations would have a variety of implications. For example, definite correlations between variations in Aβ fibril structures and variations in the severity of cognitive impairment or progression rate of AD would support the idea that fibrils are not devoid of clinically significant neurotoxic effects (Chételat et al., 2012). One argument against a significant role for Aβ fibrils in AD stems from observations that variations in cognitive impairment do not correlate strongly with variations in the total quantity of amyloid material in cortical tissue in AD patients (Giannakopoulos et al., 2003) and that amyloid can develop in asymptomatic elderly people in quantities similar to (but generally less than) those in patients with AD (Aizenstein et al., 2008). This argument does not take into account the fact that different predominant Aβ fibril structures can develop in different patients (Lu et al., 2013), which may have different neurotoxic and cognitive effects.

Correlations between variations in amyloid fibril structure and patient-to-patient variations in neurodegenerative diseases would make the development of structure-specific amyloid imaging agents an important goal. Compounds for positron emission tomography (PET) that bind to Aβ plaques are now used in research and clinical practice (Fleisher et al., 2011; Klunk et al., 2004). The molecular-level binding sites for these compounds have not yet been identified. For Pittsburgh Compound B, the number of high-affinity binding sites per Aβ molecule has been reported to be greater than 0.5 for Aβ deposits in human brain tissue, but approximately 0.001 for Aβ deposits in Tg mouse brains and less than 0.001 for synthetic Aβ fibrils (Klunk et al., 2005). If certain Aβ40 and Aβ42 fibril structures are found in patients who experience progression from mild cognitive impairment (MCI) to AD, whereas other structures are found in patients with non-progressing MCI or in asymptomatic elderly people, then PET scanning agents that bind selectively to the AD-related structures would be highly desirable.

Finally, although it may be difficult to prevent the age-related accumulation of Aβ fibrils and other aggregates in brain tissue, it is conceivable that compounds can be developed to direct the aggregation process away from specific structures and toward others. If certain structures lead to neurodegeneration most aggressively, then compounds that prevent formation of those specific structures could be used to prevent or limit neurodegeneration.

ACKNOWLEDGMENTS

This work has been supported by the intramural research program of the National Institute of Diabetes and Digestive and Kidney Diseases, a component of the National Institutes of Health. I thank Drs. Zhiping Jiang and Jennifer C. Lee of the National Heart, Lung, and Blood Institute for providing the TEM image of recombinant α-synuclein fibrils in Figure 1C.

REFERENCES

Ahmed, M., Davis, J., Aucoin, D., Sato, T., Ahuja, S., Aimoto, S., Elliott, J.I., Van Nostrand, W.E., and Smith, S.O. (2010). Structural conversion of neurotoxic amyloid-β(1-42) oligomers to fibrils. Nat. Struct. Mol. Biol. *17*, 561–567.

Aizenstein, H.J., Nebes, R.D., Saxton, J.A., Price, J.C., Mathis, C.A., Tsopelas, N.D., Ziolko, S.K., James, J.A., Snitz, B.E., Houck, P.R., et al. (2008). Frequent amyloid deposition without significant cognitive impairment among the elderly. Arch. Neurol. *65*, 1509–1517.

Andronesi, O.C., von Bergen, M., Biernat, J., Seidel, K., Griesinger, C., Mandelkow, E., and Baldus, M. (2008). Characterization of Alzheimer's-like paired helical filaments from the core domain of tau protein using solid-state NMR spectroscopy. J. Am. Chem. Soc. *130*, 5922–5928.

Antzutkin, O.N., Balbach, J.J., Leapman, R.D., Rizzo, N.W., Reed, J., and Tycko, R. (2000). Multiple quantum solid-state NMR indicates a parallel, not antiparallel, organization of β-sheets in Alzheimer's β-amyloid fibrils. Proc. Natl. Acad. Sci. USA *97*, 13045–13050.

Antzutkin, O.N., Leapman, R.D., Balbach, J.J., and Tycko, R. (2002). Supramolecular structural constraints on Alzheimer's β-amyloid fibrils from electron microscopy and solid-state nuclear magnetic resonance. Biochemistry *41*, 15436–15450.

Aoyagi, H., Hasegawa, M., and Tamaoka, A. (2007). Fibrillogenic nuclei composed of P301L mutant tau induce elongation of P301L tau but not wild-type tau. J. Biol. Chem. *282*, 20309–20318.

Ashe, K.H., and Aguzzi, A. (2013). Prions, prionoids and pathogenic proteins in Alzheimer disease. Prion *7*, 55–59.

Balbach, J.J., Petkova, A.T., Oyler, N.A., Antzutkin, O.N., Gordon, D.J., Meredith, S.C., and Tycko, R. (2002). Supramolecular structure in full-length Alzheimer's β-amyloid fibrils: evidence for a parallel β-sheet organization from solid-state nuclear magnetic resonance. Biophys. J. *83*, 1205–1216.

Bedrood, S., Li, Y., Isas, J.M., Hegde, B.G., Baxa, U., Haworth, I.S., and Langen, R. (2012). Fibril structure of human islet amyloid polypeptide. J. Biol. Chem. *287*, 5235–5241.

Benzinger, T.L.S., Gregory, D.M., Burkoth, T.S., Miller-Auer, H., Lynn, D.G., Botto, R.E., and Meredith, S.C. (1998). Propagating structure of Alzheimer's β-amyloid(10-35) is parallel β-sheet with residues in exact register. Proc. Natl. Acad. Sci. USA *95*, 13407–13412.

Bertini, I., Gonnelli, L., Luchinat, C., Mao, J., and Nesi, A. (2011). A new structural model of Aβ40 fibrils. J. Am. Chem. Soc. *133*, 16013–16022.

Bousset, L., Pieri, L., Ruiz-Arlandis, G., Gath, J., Jensen, P.H., Habenstein, B., Madiona, K., Olieric, V., Böckmann, A., Meier, B.H., and Melki, R. (2013). Structural and functional characterization of two α-synuclein strains. Nat. Commun. *4*, 2575.

Caughey, B., Raymond, G.J., and Bessen, R.A. (1998). Strain-dependent differences in β-sheet conformations of abnormal prion protein. J. Biol. Chem. *273*, 32230–32235.

Chen, S., Ferrone, F.A., and Wetzel, R. (2002). Huntington's disease age-of-onset linked to polyglutamine aggregation nucleation. Proc. Natl. Acad. Sci. USA *99*, 11884–11889.

Chen, M., Margittai, M., Chen, J., and Langen, R. (2007). Investigation of α-synuclein fibril structure by site-directed spin labeling. J. Biol. Chem. *282*, 24970–24979.

Chételat, G., Villemagne, V.L., Villain, N., Jones, G., Ellis, K.A., Ames, D., Martins, R.N., Masters, C.L., Rowe, C.C., and Grp, A.R.; AIBL Research Group (2012). Accelerated cortical atrophy in cognitively normal elderly with high β-amyloid deposition. Neurology *78*, 477–484.

Chimon, S., and Ishii, Y. (2005). Capturing intermediate structures of Alzheimer's β-amyloid, Abeta(1-40), by solid-state NMR spectroscopy. J. Am. Chem. Soc. *127*, 13472–13473.

Chimon, S., Shaibat, M.A., Jones, C.R., Calero, D.C., Aizezi, B., and Ishii, Y. (2007). Evidence of fibril-like β-sheet structures in a neurotoxic amyloid intermediate of Alzheimer's β-amyloid. Nat. Struct. Mol. Biol. *14*, 1157–1164.

Clavaguera, F., Akatsu, H., Fraser, G., Crowther, R.A., Frank, S., Hench, J., Probst, A., Winkler, D.T., Reichwald, J., Staufenbiel, M., et al. (2013). Brain homogenates from human tauopathies induce tau inclusions in mouse brain. Proc. Natl. Acad. Sci. USA *110*, 9535–9540.

Cobb, N.J., Sönnichsen, F.D., McHaourab, H., and Surewicz, W.K. (2007). Molecular architecture of human prion protein amyloid: a parallel, in-register β-structure. Proc. Natl. Acad. Sci. USA *104*, 18946–18951.

Cohen, S.I.A., Linse, S., Luheshi, L.M., Hellstrand, E., White, D.A., Rajah, L., Otzen, D.E., Vendruscolo, M., Dobson, C.M., and Knowles, T.P.J. (2013). Proliferation of amyloid-β42 aggregates occurs through a secondary nucleation mechanism. Proc. Natl. Acad. Sci. USA *110*, 9758–9763.

Collinge, J., and Clarke, A.R. (2007). A general model of prion strains and their pathogenicity. Science *318*, 930–936.

Comellas, G., Lemkau, L.R., Nieuwkoop, A.J., Kloepper, K.D., Ladror, D.T., Ebisu, R., Woods, W.S., Lipton, A.S., George, J.M., and Rienstra, C.M. (2011). Structured regions of α-synuclein fibrils include the early-onset Parkinson's disease mutation sites. J. Mol. Biol. *411*, 881–895.

Cunningham, C. (2013). Microglia and neurodegeneration: the role of systemic inflammation. Glia *61*, 71–90.

Daebel, V., Chinnathambi, S., Biernat, J., Schwalbe, M., Habenstein, B., Loquet, A., Akoury, E., Tepper, K., Müller, H., Baldus, M., et al. (2012). β-Sheet core of tau paired helical filaments revealed by solid-state NMR. J. Am. Chem. Soc. *134*, 13982–13989.

De Paëpe, G. (2012). Dipolar recoupling in magic angle spinning solid-state nuclear magnetic resonance. Annu. Rev. Phys. Chem. *63*, 661–684.

Der-Sarkissian, A., Jao, C.C., Chen, J., and Langen, R. (2003). Structural organization of α-synuclein fibrils studied by site-directed spin labeling. J. Biol. Chem. *278*, 37530–37535.

Dickson, D.W., Ahmed, Z., Algom, A.A., Tsuboi, Y., and Josephs, K.A. (2010). Neuropathology of variants of progressive supranuclear palsy. Curr. Opin. Neurol. *23*, 394–400.

Eanes, E.D., and Glenner, G.G. (1968). X-ray diffraction studies on amyloid filaments. J. Histochem. Cytochem. *16*, 673–677.

Eisele, Y.S., Obermüller, U., Heilbronner, G., Baumann, F., Kaeser, S.A., Wolburg, H., Walker, L.C., Staufenbiel, M., Heikenwalder, M., and Jucker, M. (2010). Peripherally applied Abeta-containing inoculates induce cerebral β-amyloidosis. Science *330*, 980–982.

Eskici, G., and Axelsen, P.H. (2012). Copper and oxidative stress in the pathogenesis of Alzheimer's disease. Biochemistry *51*, 6289–6311.

Estrada, L.D., and Soto, C. (2007). Disrupting β-amyloid aggregation for Alzheimer disease treatment. Curr. Top. Med. Chem. *7*, 115–126.

Fleisher, A.S., Chen, K., Liu, X., Roontiva, A., Thiyyagura, P., Ayutyanont, N., Joshi, A.D., Clark, C.M., Mintun, M.A., Pontecorvo, M.J., et al. (2011). Using positron emission tomography and florbetapir F18 to image cortical amyloid in patients with mild cognitive impairment or dementia due to Alzheimer disease. Arch. Neurol. *68*, 1404–1411.

Franks, W.T., Wylie, B.J., Schmidt, H.L.F., Nieuwkoop, A.J., Mayrhofer, R.M., Shah, G.J., Graesser, D.T., and Rienstra, C.M. (2008). Dipole tensor-based atomic-resolution structure determination of a nanocrystalline protein by solid-state NMR. Proc. Natl. Acad. Sci. USA *105*, 4621–4626.

Frederick, K.K., Debelouchina, G.T., Kayatekin, C., Dorminy, T., Jacavone, A.C., Griffin, R.G., and Lindquist, S. (2014). Distinct prion strains are defined by amyloid core structure and chaperone binding site dynamics. Chem. Biol. *21*, 295–305.

Frost, B., Jacks, R.L., and Diamond, M.I. (2009a). Propagation of tau misfolding from the outside to the inside of a cell. J. Biol. Chem. *284*, 12845–12852.

Frost, B., Ollesch, J., Wille, H., and Diamond, M.I. (2009b). Conformational diversity of wild-type Tau fibrils specified by templated conformation change. J. Biol. Chem. *284*, 3546–3551.

Gath, J., Bousset, L., Habenstein, B., Melki, R., Böckmann, A., and Meier, B.H. (2014). Unlike twins: an NMR comparison of two α-synuclein polymorphs featuring different toxicity. PLoS ONE *9*, e90659.

Giannakopoulos, P., Herrmann, F.R., Bussière, T., Bouras, C., Kövari, E., Perl, D.P., Morrison, J.H., Gold, G., and Hof, P.R. (2003). Tangle and neuron numbers, but not amyloid load, predict cognitive status in Alzheimer's disease. Neurology *60*, 1495–1500.

Giasson, B.I., Forman, M.S., Higuchi, M., Golbe, L.I., Graves, C.L., Kotzbauer, P.T., Trojanowski, J.Q., and Lee, V.M.Y. (2003). Initiation and synergistic fibrillization of tau and α-synuclein. Science *300*, 636–640.

Goldsbury, C., Frey, P., Olivieri, V., Aebi, U., and Müller, S.A. (2005). Multiple assembly pathways underlie amyloid-β fibril polymorphisms. J. Mol. Biol. *352*, 282–298.

Gravina, S.A., Ho, L., Eckman, C.B., Long, K.E., Otvos, L., Jr., Younkin, L.H., Suzuki, N., and Younkin, S.G. (1995). Amyloid β protein (A β) in Alzheimer's disease brain. Biochemical and immunocytochemical analysis with antibodies specific for forms ending at A β 40 or A β 42(43). J. Biol. Chem. *270*, 7013–7016.

Guo, J.L., and Lee, V.M.Y. (2014). Cell-to-cell transmission of pathogenic proteins in neurodegenerative diseases. Nat. Med. *20*, 130–138.

Guo, J.L., Covell, D.J., Daniels, J.P., Iba, M., Stieber, A., Zhang, B., Riddle, D.M., Kwong, L.K., Xu, Y., Trojanowski, J.Q., and Lee, V.M.Y. (2013). Distinct α-synuclein strains differentially promote tau inclusions in neurons. Cell *154*, 103–117.

Hardy, J., and Revesz, T. (2012). The spread of neurodegenerative disease. N. Engl. J. Med. *366*, 2126–2128.

Heise, H., Hoyer, W., Becker, S., Andronesi, O.C., Riedel, D., and Baldus, M. (2005). Molecular-level secondary structure, polymorphism, and dynamics of full-length α-synuclein fibrils studied by solid-state NMR. Proc. Natl. Acad. Sci. USA *102*, 15871–15876.

Heise, H., Celej, M.S., Becker, S., Riedel, D., Pelah, A., Kumar, A., Jovin, T.M., and Baldus, M. (2008). Solid-state NMR reveals structural differences between fibrils of wild-type and disease-related A53T mutant α-synuclein. J. Mol. Biol. *380*, 444–450.

Helmus, J.J., Surewicz, K., Nadaud, P.S., Surewicz, W.K., and Jaroniec, C.P. (2008). Molecular conformation and dynamics of the Y145Stop variant of human prion protein in amyloid fibrils. Proc. Natl. Acad. Sci. USA *105*, 6284–6289.

Helmus, J.J., Surewicz, K., Surewicz, W.K., and Jaroniec, C.P. (2010). Conformational flexibility of Y145Stop human prion protein amyloid fibrils probed by solid-state nuclear magnetic resonance spectroscopy. J. Am. Chem. Soc. *132*, 2393–2403.

Helmus, J.J., Surewicz, K., Apostol, M.I., Surewicz, W.K., and Jaroniec, C.P. (2011). Intermolecular alignment in Y145Stop human prion protein amyloid fibrils probed by solid-state NMR spectroscopy. J. Am. Chem. Soc. *133*, 13934–13937.

Hoshi, M., Sato, M., Matsumoto, S., Noguchi, A., Yasutake, K., Yoshida, N., and Sato, K. (2003). Spherical aggregates of β-amyloid (amylospheroid) show high neurotoxicity and activate tau protein kinase I/glycogen synthase kinase-3β. Proc. Natl. Acad. Sci. USA *100*, 6370–6375.

Hoyer, W., Grönwall, C., Jonsson, A., Ståhl, S., and Härd, T. (2008). Stabilization of a β-hairpin in monomeric Alzheimer's amyloid-β peptide inhibits amyloid formation. Proc. Natl. Acad. Sci. USA *105*, 5099–5104.

Hughes, A.J., Daniel, S.E., Blankson, S., and Lees, A.J. (1993). A clinicopathologic study of 100 cases of Parkinson's disease. Arch. Neurol. *50*, 140–148.

Iba, M., Guo, J.L., McBride, J.D., Zhang, B., Trojanowski, J.Q., and Lee, V.M.Y. (2013). Synthetic tau fibrils mediate transmission of neurofibrillary tangles in a transgenic mouse model of Alzheimer's-like tauopathy. J. Neurosci. *33*, 1024–1037.

Jiménez, J.L., Guijarro, J.I., Orlova, E., Zurdo, J., Dobson, C.M., Sunde, M., and Saibil, H.R. (1999). Cryo-electron microscopy structure of an SH3 amyloid fibril and model of the molecular packing. EMBO J. *18*, 815–821.

Jones, E.M., and Surewicz, W.K. (2005). Fibril conformation as the basis of species- and strain-dependent seeding specificity of mammalian prion amyloids. Cell *121*, 63–72.

Jucker, M., and Walker, L.C. (2013). Self-propagation of pathogenic protein aggregates in neurodegenerative diseases. Nature *501*, 45–51.

Karantzoulis, S., and Galvin, J.E. (2011). Distinguishing Alzheimer's disease from other major forms of dementia. Expert Rev. Neurother. *11*, 1579–1591.

Kayed, R., Head, E., Thompson, J.L., McIntire, T.M., Milton, S.C., Cotman, C.W., and Glabe, C.G. (2003). Common structure of soluble amyloid oligomers implies common mechanism of pathogenesis. Science *300*, 486–489.

Kfoury, N., Holmes, B.B., Jiang, H., Holtzman, D.M., and Diamond, M.I. (2012). Trans-cellular propagation of Tau aggregation by fibrillar species. J. Biol. Chem. *287*, 19440–19451.

Kheterpal, I., Chen, M., Cook, K.D., and Wetzel, R. (2006). Structural differences in Abeta amyloid protofibrils and fibrils mapped by hydrogen exchange—mass spectrometry with on-line proteolytic fragmentation. J. Mol. Biol. *361*, 785–795.

Klunk, W.E., Engler, H., Nordberg, A., Wang, Y., Blomqvist, G., Holt, D.P., Bergström, M., Savitcheva, I., Huang, G.F., Estrada, S., et al. (2004). Imaging brain amyloid in Alzheimer's disease with Pittsburgh Compound-B. Ann. Neurol. *55*, 306–319.

Klunk, W.E., Lopresti, B.J., Ikonomovic, M.D., Lefterov, I.M., Koldamova, R.P., Abrahamson, E.E., Debnath, M.L., Holt, D.P., Huang, G.F., Shao, L., et al. (2005). Binding of the positron emission tomography tracer Pittsburgh compound-B reflects the amount of amyloid-β in Alzheimer's disease brain but not in transgenic mouse brain. J. Neurosci. *25*, 10598–10606.

Knowles, T.P.J., Waudby, C.A., Devlin, G.L., Cohen, S.I.A., Aguzzi, A., Vendruscolo, M., Terentjev, E.M., Welland, M.E., and Dobson, C.M. (2009). An analytical solution to the kinetics of breakable filament assembly. Science *326*, 1533–1537.

Kodali, R., Williams, A.D., Chemuru, S., and Wetzel, R. (2010). Abeta(1-40) forms five distinct amyloid structures whose β-sheet contents and fibril stabilities are correlated. J. Mol. Biol. *401*, 503–517.

Kryndushkin, D.S., Wickner, R.B., and Tycko, R. (2011). The core of Ure2p prion fibrils is formed by the N-terminal segment in a parallel cross-β structure: evidence from solid-state NMR. J. Mol. Biol. *409*, 263–277.

Ladiwala, A.R.A., Litt, J., Kane, R.S., Aucoin, D.S., Smith, S.O., Ranjan, S., Davis, J., Van Nostrand, W.E., and Tessier, P.M. (2012). Conformational differences between two amyloid β oligomers of similar size and dissimilar toxicity. J. Biol. Chem. *287*, 24765–24773.

Ladner, C.L., Chen, M., Smith, D.P., Platt, G.W., Radford, S.E., and Langen, R. (2010). Stacked sets of parallel, in-register β-strands of β2-microglobulin in amyloid fibrils revealed by site-directed spin labeling and chemical labeling. J. Biol. Chem. *285*, 17137–17147.

Laganowsky, A., Liu, C., Sawaya, M.R., Whitelegge, J.P., Park, J., Zhao, M., Pensalfini, A., Soriaga, A.B., Landau, M., Teng, P.K., et al. (2012). Atomic view of a toxic amyloid small oligomer. Science *335*, 1228–1231.

Lam, B., Masellis, M., Freedman, M., Stuss, D.T., and Black, S.E. (2013). Clinical, imaging, and pathological heterogeneity of the Alzheimer's disease syndrome. Alzheimers Res. Ther. *5*, 1.

Langer, F., Eisele, Y.S., Fritschi, S.K., Staufenbiel, M., Walker, L.C., and Jucker, M. (2011). Soluble Aβ seeds are potent inducers of cerebral β-amyloid deposition. J. Neurosci. *31*, 14488–14495.

Lansbury, P.T., Jr., Costa, P.R., Griffiths, J.M., Simon, E.J., Auger, M., Halverson, K.J., Kocisko, D.A., Hendsch, Z.S., Ashburn, T.T., Spencer, R.G.S., et al. (1995). Structural model for the β-amyloid fibril based on interstrand alignment of an antiparallel-sheet comprising a C-terminal peptide. Nat. Struct. Biol. *2*, 990–998.

Lasagna-Reeves, C.A., Glabe, C.G., and Kayed, R. (2011). Amyloid-β annular protofibrils evade fibrillar fate in Alzheimer disease brain. J. Biol. Chem. *286*, 22122–22130.

Lemkau, L.R., Comellas, G., Kloepper, K.D., Woods, W.S., George, J.M., and Rienstra, C.M. (2012). Mutant protein A30P α-synuclein adopts wild-type fibril structure, despite slower fibrillation kinetics. J. Biol. Chem. *287*, 11526–11532.

Lemkau, L.R., Comellas, G., Lee, S.W., Rikardsen, L.K., Woods, W.S., George, J.M., and Rienstra, C.M. (2013). Site-specific perturbations of α-synuclein fibril structure by the Parkinson's disease associated mutations A53T and E46K. PLoS ONE *8*, e49750.

Lesné, S., Koh, M.T., Kotilinek, L., Kayed, R., Glabe, C.G., Yang, A., Gallagher, M., and Ashe, K.H. (2006). A specific amyloid-β protein assembly in the brain impairs memory. Nature *440*, 352–357.

Lesné, S.E., Sherman, M.A., Grant, M., Kuskowski, M., Schneider, J.A., Bennett, D.A., and Ashe, K.H. (2013). Brain amyloid-β oligomers in ageing and Alzheimer's disease. Brain *136*, 1383–1398.

Li, S., Hong, S., Shepardson, N.E., Walsh, D.M., Shankar, G.M., and Selkoe, D. (2009). Soluble oligomers of amyloid β protein facilitate hippocampal long-term depression by disrupting neuronal glutamate uptake. Neuron *62*, 788–801.

Lomakin, A., Teplow, D.B., Kirschner, D.A., and Benedek, G.B. (1997). Kinetic theory of fibrillogenesis of amyloid β-protein. Proc. Natl. Acad. Sci. USA *94*, 7942–7947.

Lopez del Amo, J.M., Fink, U., Dasari, M., Grelle, G., Wanker, E.E., Bieschke, J., and Reif, B. (2012). Structural properties of EGCG-induced, nontoxic Alzheimer's disease Aβ oligomers. J. Mol. Biol. *421*, 517–524.

Lu, J.X., Qiang, W., Yau, W.M., Schwieters, C.D., Meredith, S.C., and Tycko, R. (2013). Molecular structure of β-amyloid fibrils in Alzheimer's disease brain tissue. Cell *154*, 1257–1268.

Luca, S., Yau, W.M., Leapman, R., and Tycko, R. (2007). Peptide conformation and supramolecular organization in amylin fibrils: constraints from solid-state NMR. Biochemistry *46*, 13505–13522.

Lührs, T., Ritter, C., Adrian, M., Riek-Loher, D., Bohrmann, B., Döbeli, H., Schubert, D., and Riek, R. (2005). 3D structure of Alzheimer's amyloid-β(1-42) fibrils. Proc. Natl. Acad. Sci. USA *102*, 17342–17347.

Luk, K.C., Kehm, V., Carroll, J., Zhang, B., O'Brien, P., Trojanowski, J.Q., and Lee, V.M.Y. (2012a). Pathological α-synuclein transmission initiates Parkinson-like neurodegeneration in nontransgenic mice. Science *338*, 949–953.

Luk, K.C., Kehm, V.M., Zhang, B., O'Brien, P., Trojanowski, J.Q., and Lee, V.M.Y. (2012b). Intracerebral inoculation of pathological α-synuclein initiates a rapidly progressive neurodegenerative α-synucleinopathy in mice. J. Exp. Med. *209*, 975–986.

Margittai, M., and Langen, R. (2004). Template-assisted filament growth by parallel stacking of tau. Proc. Natl. Acad. Sci. USA *101*, 10278–10283.

Margittai, M., and Langen, R. (2008). Fibrils with parallel in-register structure constitute a major class of amyloid fibrils: molecular insights from electron paramagnetic resonance spectroscopy. Q. Rev. Biophys. *41*, 265–297.

Meinhardt, J., Sachse, C., Hortschansky, P., Grigorieff, N., and Fändrich, M. (2009). Abeta(1-40) fibril polymorphism implies diverse interaction patterns in amyloid fibrils. J. Mol. Biol. *386*, 869–877.

Meyer-Luehmann, M., Coomaraswamy, J., Bolmont, T., Kaeser, S., Schaefer, C., Kilger, E., Neuenschwander, A., Abramowski, D., Frey, P., Jaton, A.L., et al. (2006). Exogenous induction of cerebral β-amyloidogenesis is governed by agent and host. Science *313*, 1781–1784.

Morales, R., Duran-Aniotz, C., Castilla, J., Estrada, L.D., and Soto, C. (2012). De novo induction of amyloid-β deposition in vivo. Mol. Psychiatry *17*, 1347–1353.

Nelson, R., Sawaya, M.R., Balbirnie, M., Madsen, A.O., Riekel, C., Grothe, R., and Eisenberg, D. (2005). Structure of the cross-β spine of amyloid-like fibrils. Nature *435*, 773–778.

Nicoll, A.J., Panico, S., Freir, D.B., Wright, D., Terry, C., Risse, E., Herron, C.E., O'Malley, T., Wadsworth, J.D.F., Farrow, M.A., et al. (2013). Amyloid-β nanotubes are associated with prion protein-dependent synaptotoxicity. Nat. Commun. *4*, 2416.

Niu, Z., Zhao, W., Zhang, Z., Xiao, F., Tang, X., and Yang, J. (2014). The molecular structure of Alzheimer β-amyloid fibrils formed in the presence of phospholipid vesicles. Angew. Chem. Int. Ed. Engl. *53*, 9294–9297.

Noguchi, A., Matsumura, S., Dezawa, M., Tada, M., Yanazawa, M., Ito, A., Akioka, M., Kikuchi, S., Sato, M., Ideno, S., et al. (2009). Isolation and characterization of patient-derived, toxic, high mass amyloid β-protein (Abeta) assembly from Alzheimer disease brains. J. Biol. Chem. *284*, 32895–32905.

O'Nuallain, B., Williams, A.D., Westermark, P., and Wetzel, R. (2004). Seeding specificity in amyloid growth induced by heterologous fibrils. J. Biol. Chem. *279*, 17490–17499.

Olofsson, A., Lindhagen-Persson, M., Sauer-Eriksson, A.E., and Ohman, A. (2007). Amide solvent protection analysis demonstrates that amyloid-β(1-40) and amyloid-β(1-42) form different fibrillar structures under identical conditions. Biochem. J. *404*, 63–70.

Paravastu, A.K., Leapman, R.D., Yau, W.M., and Tycko, R. (2008). Molecular structural basis for polymorphism in Alzheimer's β-amyloid fibrils. Proc. Natl. Acad. Sci. USA *105*, 18349–18354.

Paravastu, A.K., Qahwash, I., Leapman, R.D., Meredith, S.C., and Tycko, R. (2009). Seeded growth of β-amyloid fibrils from Alzheimer's brain-derived fibrils produces a distinct fibril structure. Proc. Natl. Acad. Sci. USA *106*, 7443–7448.

Petkova, A.T., Leapman, R.D., Guo, Z., Yau, W.M., Mattson, M.P., and Tycko, R. (2005). Self-propagating, molecular-level polymorphism in Alzheimer's β-amyloid fibrils. Science *307*, 262–265.

Petkova, A.T., Yau, W.M., and Tycko, R. (2006). Experimental constraints on quaternary structure in Alzheimer's β-amyloid fibrils. Biochemistry *45*, 498–512.

Pham, C.L.L., Kwan, A.H., and Sunde, M. (2014). Functional amyloid: widespread in nature, diverse in purpose. Essays Biochem. *56*, 207–219.

Prusiner, S.B. (2013). Biology and genetics of prions causing neurodegeneration. Annu. Rev. Genet. *47*, 601–623.

Qiang, W., Yau, W.M., and Tycko, R. (2011). Structural evolution of Iowa mutant β-amyloid fibrils from polymorphic to homogeneous states under repeated seeded growth. J. Am. Chem. Soc. *133*, 4018–4029.

Qiang, W., Yau, W.M., Luo, Y., Mattson, M.P., and Tycko, R. (2012). Antiparallel β-sheet architecture in Iowa-mutant β-amyloid fibrils. Proc. Natl. Acad. Sci. USA *109*, 4443–4448.

Qiang, W., Kelley, K., and Tycko, R. (2013). Polymorph-specific kinetics and thermodynamics of β-amyloid fibril growth. J. Am. Chem. Soc. *135*, 6860–6871.

Resende, R., Ferreiro, E., Pereira, C., and Resende de Oliveira, C. (2008). Neurotoxic effect of oligomeric and fibrillar species of amyloid-β peptide 1-42: involvement of endoplasmic reticulum calcium release in oligomer-induced cell death. Neuroscience *155*, 725–737.

Rosen, R.F., Fritz, J.J., Dooyema, J., Cintron, A.F., Hamaguchi, T., Lah, J.J., LeVine, H., 3rd, Jucker, M., and Walker, L.C. (2012). Exogenous seeding of cerebral β-amyloid deposition in βAPP-transgenic rats. J. Neurochem. *120*, 660–666.

Safar, J., Wille, H., Itri, V., Groth, D., Serban, H., Torchia, M., Cohen, F.E., and Prusiner, S.B. (1998). Eight prion strains have $PrP^{(Sc)}$ molecules with different conformations. Nat. Med. *4*, 1157–1165.

Sandberg, A., Luheshi, L.M., Söllvander, S., Pereira de Barros, T., Macao, B., Knowles, T.P.J., Biverstål, H., Lendel, C., Ekholm-Petterson, F., Dubnovitsky, A., et al. (2010). Stabilization of neurotoxic Alzheimer amyloid-β oligomers by protein engineering. Proc. Natl. Acad. Sci. USA *107*, 15595–15600.

Sanders, D.W., Kaufman, S.K., DeVos, S.L., Sharma, A.M., Mirbaha, H., Li, A., Barker, S.J., Foley, A.C., Thorpe, J.R., Serpell, L.C., et al. (2014). Distinct tau prion strains propagate in cells and mice and define different tauopathies. Neuron *82*, 1271–1288.

Sarkar, B., Mithu, V.S., Chandra, B., Mandal, A., Chandrakesan, M., Bhowmik, D., Madhu, P.K., and Maiti, S. (2014). Significant structural differences between transient amyloid-β oligomers and less-toxic fibrils in regions known to harbor familial Alzheimer's mutations. Angew. Chem. Int. Ed. Engl. *53*, 6888–6892.

Sato, T., Kienlen-Campard, P., Ahmed, M., Liu, W., Li, H., Elliott, J.I., Aimoto, S., Constantinescu, S.N., Octave, J.N., and Smith, S.O. (2006). Inhibitors of amyloid toxicity based on β-sheet packing of Abeta40 and Abeta42. Biochemistry *45*, 5503–5516.

Sawaya, M.R., Sambashivan, S., Nelson, R., Ivanova, M.I., Sievers, S.A., Apostol, M.I., Thompson, M.J., Balbirnie, M., Wiltzius, J.J.W., McFarlane, H.T., et al. (2007). Atomic structures of amyloid cross-β spines reveal varied steric zippers. Nature *447*, 453–457.

Scheidt, H.A., Morgado, I., Rothemund, S., Huster, D., and Fändrich, M. (2011). Solid-state NMR spectroscopic investigation of Aβ protofibrils: implication of a β-sheet remodeling upon maturation into terminal amyloid fibrils. Angew. Chem. Int. Ed. Engl. *50*, 2837–2840.

Scheidt, H.A., Morgado, I., and Huster, D. (2012). Solid-state NMR reveals a close structural relationship between amyloid-β protofibrils and oligomers. J. Biol. Chem. *287*, 22822–22826.

Schneider, J.A., Watts, R.L., Gearing, M., Brewer, R.P., and Mirra, S.S. (1997). Corticobasal degeneration: neuropathologic and clinical heterogeneity. Neurology *48*, 959–969.

Schutz, A.K., Vagt, T., Huber, M., Ovchinnikova, O.Y., Cadalbert, R., Wall, J., Guntert, P., Bockmann, A., Glockshuber, R., and Meier, B.H. (2014). Atomic-resolution three-dimensional structure of amyloid-β fibrils bearing the Osaka mutation. Angew. Chem. Int. Ed. *53*, 1–6.

Sengupta, I., Nadaud, P.S., and Jaroniec, C.P. (2013). Protein structure determination with paramagnetic solid-state NMR spectroscopy. Acc. Chem. Res. *46*, 2117–2126.

Serpell, L.C., and Smith, J.M. (2000). Direct visualisation of the β-sheet structure of synthetic Alzheimer's amyloid. J. Mol. Biol. *299*, 225–231.

Shankar, G.M., Li, S., Mehta, T.H., Garcia-Munoz, A., Shepardson, N.E., Smith, I., Brett, F.M., Farrell, M.A., Rowan, M.J., Lemere, C.A., et al. (2008). Amyloid-β protein dimers isolated directly from Alzheimer's brains impair synaptic plasticity and memory. Nat. Med. *14*, 837–842.

Shen, Y., Delaglio, F., Cornilescu, G., and Bax, A. (2009). TALOS+: a hybrid method for predicting protein backbone torsion angles from NMR chemical shifts. J. Biomol. NMR *44*, 213–223.

Shewmaker, F., Wickner, R.B., and Tycko, R. (2006). Amyloid of the prion domain of Sup35p has an in-register parallel β-sheet structure. Proc. Natl. Acad. Sci. USA *103*, 19754–19759.

Spies, P.E., Slats, D., Sjögren, J.M.C., Kremer, B.P.H., Verhey, F.R.J., Rikkert, M.G., and Verbeek, M.M. (2010). The cerebrospinal fluid amyloid β42/40 ratio in the differentiation of Alzheimer's disease from non-Alzheimer's dementia. Curr. Alzheimer Res. *7*, 470–476.

Stöhr, J., Watts, J.C., Mensinger, Z.L., Oehler, A., Grillo, S.K., DeArmond, S.J., Prusiner, S.B., and Giles, K. (2012). Purified and synthetic Alzheimer's amyloid beta (Aβ) prions. Proc. Natl. Acad. Sci. USA *109*, 11025–11030.

Stöhr, J., Condello, C., Watts, J.C., Bloch, L., Oehler, A., Nick, M., DeArmond, S.J., Giles, K., DeGrado, W.F., and Prusiner, S.B. (2014). Distinct synthetic Aβ prion strains producing different amyloid deposits in bigenic mice. Proc. Natl. Acad. Sci. USA *111*, 10329–10334.

Sunde, M., Serpell, L.C., Bartlam, M., Fraser, P.E., Pepys, M.B., and Blake, C.C.F. (1997). Common core structure of amyloid fibrils by synchrotron X-ray diffraction. J. Mol. Biol. *273*, 729–739.

Tay, W.M., Huang, D., Rosenberry, T.L., and Paravastu, A.K. (2013). The Alzheimer's amyloid-β(1-42) peptide forms off-pathway oligomers and fibrils that are distinguished structurally by intermolecular organization. J. Mol. Biol. *425*, 2494–2508.

Taylor, K.L., Cheng, N., Williams, R.W., Steven, A.C., and Wickner, R.B. (1999). Prion domain initiation of amyloid formation in vitro from native Ure2p. Science *283*, 1339–1343.

Telling, G.C., Parchi, P., DeArmond, S.J., Cortelli, P., Montagna, P., Gabizon, R., Mastrianni, J., Lugaresi, E., Gambetti, P., and Prusiner, S.B. (1996). Evidence for the conformation of the pathologic isoform of the prion protein enciphering and propagating prion diversity. Science *274*, 2079–2082.

Thal, D.R., Rüb, U., Orantes, M., and Braak, H. (2002). Phases of A β-deposition in the human brain and its relevance for the development of AD. Neurology *58*, 1791–1800.

Tomic, J.L., Pensalfini, A., Head, E., and Glabe, C.G. (2009). Soluble fibrillar oligomer levels are elevated in Alzheimer's disease brain and correlate with cognitive dysfunction. Neurobiol. Dis. *35*, 352–358.

Török, M., Milton, S., Kayed, R., Wu, P., McIntire, T., Glabe, C.G., and Langen, R. (2002). Structural and dynamic features of Alzheimer's Abeta peptide in amyloid fibrils studied by site-directed spin labeling. J. Biol. Chem. *277*, 40810–40815.

Toyama, B.H., and Weissman, J.S. (2011). Amyloid structure: conformational diversity and consequences. Annu. Rev. Biochem. *80*, 557–585.

Toyama, B.H., Kelly, M.J.S., Gross, J.D., and Weissman, J.S. (2007). The structural basis of yeast prion strain variants. Nature *449*, 233–237.

Tycko, R. (2011). Solid-state NMR studies of amyloid fibril structure. Annu. Rev. Phys. Chem. *62*, 279–299.

Tycko, R. (2014). Physical and structural basis for polymorphism in amyloid fibrils. Protein Sci. *23*, 1528–1539.

Tycko, R., Sciarretta, K.L., Orgel, J.P., and Meredith, S.C. (2009). Evidence for novel β-sheet structures in Iowa mutant β-amyloid fibrils. Biochemistry *48*, 6072–6084.

Tycko, R., Savtchenko, R., Ostapchenko, V.G., Makarava, N., and Baskakov, I.V. (2010). The α-helical C-terminal domain of full-length recombinant PrP converts to an in-register parallel β-sheet structure in PrP fibrils: evidence from solid state nuclear magnetic resonance. Biochemistry *49*, 9488–9497.

Van Melckebeke, H., Wasmer, C., Lange, A., Ab, E., Loquet, A., Böckmann, A., and Meier, B.H. (2010). Atomic-resolution three-dimensional structure of HET-s(218-289) amyloid fibrils by solid-state NMR spectroscopy. J. Am. Chem. Soc. *132*, 13765–13775.

Volpicelli-Daley, L.A., Luk, K.C., Patel, T.P., Tanik, S.A., Riddle, D.M., Stieber, A., Meaney, D.F., Trojanowski, J.Q., and Lee, V.M.Y. (2011). Exogenous α-synuclein fibrils induce Lewy body pathology leading to synaptic dysfunction and neuron death. Neuron *72*, 57–71.

von Bergen, M., Friedhoff, P., Biernat, J., Heberle, J., Mandelkow, E.M., and Mandelkow, E. (2000). Assembly of tau protein into Alzheimer paired helical filaments depends on a local sequence motif ($(_{306}$VQIVYK$_{311})$) forming β structure. Proc. Natl. Acad. Sci. USA *97*, 5129–5134.

Walker, L.C., Diamond, M.I., Duff, K.E., and Hyman, B.T. (2013). Mechanisms of protein seeding in neurodegenerative diseases. JAMA Neurol. *70*, 304–310.

Walsh, D.M., Klyubin, I., Fadeeva, J.V., Cullen, W.K., Anwyl, R., Wolfe, M.S., Rowan, M.J., and Selkoe, D.J. (2002). Naturally secreted oligomers of amyloid β protein potently inhibit hippocampal long-term potentiation in vivo. Nature *416*, 535–539.

Watts, J.C., Condello, C., Stöhr, J., Oehler, A., Lee, J., DeArmond, S.J., Lannfelt, L., Ingelsson, M., Giles, K., and Prusiner, S.B. (2014). Serial propagation of distinct strains of Aβ prions from Alzheimer's disease patients. Proc. Natl. Acad. Sci. USA *111*, 10323–10328.

Wetzel, R. (2006). Kinetics and thermodynamics of amyloid fibril assembly. Acc. Chem. Res. *39*, 671–679.

Wickner, R.B., Dyda, F., and Tycko, R. (2008). Amyloid of Rnq1p, the basis of the [PIN+] prion, has a parallel in-register β-sheet structure. Proc. Natl. Acad. Sci. USA *105*, 2403–2408.

Wickner, R.B., Shewmaker, F., Edskes, H., Kryndushkin, D., Nemecek, J., McGlinchey, R., Bateman, D., and Winchester, C.L. (2010). Prion amyloid structure explains templating: how proteins can be genes. FEMS Yeast Res. *10*, 980–991.

Williams, A.D., Sega, M., Chen, M., Kheterpal, I., Geva, M., Berthelier, V., Kaleta, D.T., Cook, K.D., and Wetzel, R. (2005). Structural properties of Abeta protofibrils stabilized by a small molecule. Proc. Natl. Acad. Sci. USA *102*, 7115–7120.

Wu, J.W., Breydo, L., Isas, J.M., Lee, J., Kuznetsov, Y.G., Langen, R., and Glabe, C. (2010). Fibrillar oligomers nucleate the oligomerization of monomeric amyloid β but do not seed fibril formation. J. Biol. Chem. *285*, 6071–6079.

Xue, W.F., Hellewell, A.L., Gosal, W.S., Homans, S.W., Hewitt, E.W., and Radford, S.E. (2009). Fibril fragmentation enhances amyloid cytotoxicity. J. Biol. Chem. *284*, 34272–34282.

Yu, L., Edalji, R., Harlan, J.E., Holzman, T.F., Lopez, A.P., Labkovsky, B., Hillen, H., Barghorn, S., Ebert, U., Richardson, P.L., et al. (2009). Structural characterization of a soluble amyloid β-peptide oligomer. Biochemistry *48*, 1870–1877.